Supporting Information

Analysis of Equilibrium Sedimentation Analytical Ultracentrifugation of Two Dissimilar Interacting Species

As described in the main text, sedimentation equilibrium analytical ultracentrifugation data were analyzed using an approach that derives in part from previous methods for analyzing the formation of complexes by two dissimilar species, interacting at sedimentation equilibrium in an ultracentrifugal field (see references *23-26*). In SPR experiments described in the paper, 1:1 complexes were shown to form between an inhibitor peptide (I), $5QMe_2$, and the aggregating peptide (Q), $YAQ_{12}A$. When sedimentation equilibrium is attained, other equilibria will be attained as well, including the formation of the complex between I and Q. For each sedimenting species in the mixture, the concentration at each position in the ultracentrifugal field, $C_i(r)$ is given by:

$$C_i(r) = C_i(r_F)\ \psi_i(r) \qquad \text{Supp. Eq. 1}$$

where r is radial distance from the center of rotation, the function $\psi_i(r)$ is defined as :

$$\psi_i(r) = \exp[M_i\phi_i(r^2 - r_F^2)] \qquad \text{Supp. Eq. 2}$$

and

$$\phi_i = \frac{\left(1 - \bar{v}_i \rho\right)\omega^2}{2RT}$$ Supp. Eq. 3

and r_F is an arbitrarily chosen fixed radial distance from the center of rotation.

Thus, the total (or constituent) concentrations can be described as:

$$C_t(r) = C_I(r_F)\, \psi_I(r) + C_Q(r_F)\, \psi_Q(r) + C_{IQ}(r_F)\, \psi_{IQ}(r) + C_{I2Q}(r_F)\, \psi_{I2Q}(r) + \ldots$$ Supp. Eq. 4

assuming, from ideality of the solutes, that the chemical potentials of each component can be expressed in terms of the concentration.

SPR experiments demonstrated that I and Q interact with moderate affinity to form predominantly or exclusively a 1:1 complex. The above expression also allows for the occurrence of higher order complexes either of the fibril-forming peptide, the inhibitor, or both. While it is not possible to exclude the occurrence of such higher order complexes in minute quantities, the null hypothesis is that the 1:1: stoichiometric complex is the predominant species, and the ultracentrifugation data can be analyzed to determine whether these data are consistent with the null hypothesis. As shown by Nichol *et al*. and subsequent investigators (see references *23-26*), the sedimentation of all species is interdependent. Thus, if

$$\psi_Q(r) = \exp\left[\frac{M_Q\left(1 - \bar{v}_Q \rho\right)\omega^2}{2RT}\left(r^2 - r_F^2\right)\right]$$ Supp. Eq. 5

and

$$\psi_I(r) = \exp\left[\frac{M_I\left(1-\bar{v}_I\rho\right)\omega^2}{2RT}\left(r^2 - r_F^2\right)\right] \qquad \text{Supp. Eq. 6}$$

then, after dividing one expression by the other and re-arranging, it follows clearly that

$$\frac{\ln\left[\psi_Q(r)\right]}{\ln\left[\psi_I(r)\right]} = \frac{M_Q\phi_Q}{M_I\phi_I} \qquad \text{Supp. Eq. 7}$$

These authors define the above ratio as p, that is,

$$p = \frac{M_Q\phi_Q}{M_I\phi_I} \qquad \text{Supp. Eq. 8}$$

The advantage of expressing sedimentation and other equilibria in this way is that EQ. 1 can be re-written in terms of the single variable $\psi_I(r)$:

$$C_t(r) = C_I(r_F)\,\psi_I(r) + C_Q(r_F)\,[\psi_I(r)]^p + C_{IQ}(r_F)\,[\psi_I(r)]^{p+1} + C_{I2Q}(r_F)\,[\psi_I(r)]^{p+2} + \ldots \qquad \text{Supp. Eq. 9}$$

As shown in Results, from the molecular weights and partial-specific volumes of I and Q (see below for discussion of partial specific volumes), the value obtained for p is 1.90. This equation also implicitly includes the equilibrium constant for formation of the complex, IQ, since at every position in the ultracentrifugal field (considering now a 1:1 stoichiometric complex of I and Q),

$$K_d = \frac{C_I(r_F)\psi_I \cdot C_Q(r_F)\psi_Q}{C_{IQ}(r_F)\psi_{IQ}} = \frac{C_I(r_F)\psi_I \cdot C_Q(r_F)\psi_I^{\,p}}{C_{IQ}(r_F)\psi_I^{\,p+1}} = \frac{C_I(r_F) \cdot C_Q(r_F)}{C_{IQ}(r_F)}$$ Supp. Eq. 10

Thus, the four parameters, $C_I(r_F)$, $C_Q(r_F)$, $C_{IQ}(r_F)$ and K_d are related to one another, and if one can obtain any three of these parameters, the fourth can be calculated.

Experimentally, sedimentation was followed by measuring absorbance at a single wavelength, either 280 or 230 nm depending on the sensitivity needed at given concentrations of I and Q. The total absorbance due to all species at each r, $A_t(r)$, is defined as follows:

$$A_t(r) = A_I(r) + A_Q(r) + A_{IQ}(r) + A_{I2Q}(r) + \ldots$$ Supp. Eq. 11

The absorbance is related to the concentration by the equation,

$$C_t = C_I + C_Q + C_{IQ} + C_{I2Q} + \ldots$$ Supp. Eq. 12

$$C_t = A_I/\varepsilon_I + A_Q/\varepsilon_Q + A_{IQ}/\varepsilon_{IQ} + A_{I2Q}/\varepsilon_{I2Q} + \ldots$$ Supp. Eq. 13

where ε_i is the extinction coefficient of each species. Thus,

$$A_i(r) = C_i(r)\ \varepsilon_i = C_i(r_F)\ \varepsilon_i\ \psi_I(r)$$ Supp. Eq. 14

and thus from Equation 2 it follows that

$$A_t(r) = C_I(r_F)\,\varepsilon_I\,\psi_I(r) + C_Q(r_F)\,\varepsilon_Q\,[\psi_I(r)]^p + C_{IQ}(r_F)\,\varepsilon_{IQ}\,[\psi_I(r)]^{p+1} + \ldots \qquad \text{Supp. Eq. 15}$$

Supp. Eq. 15 (same as Eq. 3 in the main paper) describes the relationship between the observed total absorbance as a function of the radius. The parameters, $C_i(r_F)\varepsilon_i$, are coefficients that can be calculated from non-linear least squares analysis. Values for the extinction coefficients of I and Q were determined by measuring the absorbance of solutions of each of the two peptides at 280 nm at concentrations up to 1.5 mM, and were found to be 475 $cm^{-1}M^{-1}$ and 1010 $cm^{-1}M^{-1}$ for I and Q, respectively. The extinction coefficient of IQ was estimated as the sum of these two extinction coefficients, i.e., 1485 $cm^{-1}\ M^{-1}$.

In these experiments, sedimentation equilibrium ultracentrifugation was performed using three sets of peptide concentrations, either an equimolar concentration of I and Q (100 μM of each), or excess of the inhibitor (500 or 1000 μM of I with 100 μM of Q). In addition, the sample was centrifuged to equilibrium at three angular velocities, 36000, 48000, and 60000 rpm. It was necessary to use equimolar or higher inhibitor concentration because at lower concentrations of the inhibitor, Q would not stay in solution, as is also indicated in Figure 1 of the paper.

First, the data were analyzed using Eq. 3 (the same as Supp. Eq. 15). We first showed that the introduction of higher order terms in either I, Q, or both, did not improve the fit of the data to the equation. Supporting Figure 3 shows three lines, representing the three simplest cases: 1) only I, Q, and IQ were present. 2) I, Q, IQ, and IQ_2 were present. 3) I, Q, IQ, and I_2Q were present. The lines are entirely superimposable, indicating that the introduction of higher order terms is not required to fit the data. Applying Ockham's razor, we now consider only the

simplest of the three cases, in which there are appreciable quantities of only I, Q, and IQ, a 1:1 stoichiometric complex.

Under these conditions of equimolar or excess I compared to Q, and given the K_d (0.92 μM) obtained from SPR, the expected concentration of Q is low compared to those of either I or IQ, and also with respect to the experimental error in measurement of absorbance. For this reason, the results were analyzed in two, complementary ways. First, the value of K_d was evaluated from the values of the three parameters, $C_I(r_F)$, $C_Q(r_F)$, and $C_{IQ}(r_F)$. Second, we used the value of K_d obtained from SPR experiments to calculate the least precise (because it has the lowest value) of the above three parameters, $C_Q(r_F)$. That is, data were analyzed by non-linear least squares methods, using the equation:

$$A_t(r) = \frac{C_I(r_F)}{\varepsilon_I}\psi_I + \frac{\frac{C_I(r_F)}{\varepsilon_I}\cdot K_d}{\frac{C_{IQ}(r_F)}{\varepsilon_{IQ}}}\psi_I^{\,p} + \frac{C_{IQ}(r_F)}{\varepsilon_{IQ}}\psi_I^{\,p+1} \qquad \text{Supp. Eq. 16}$$

Figure 5 shows the results of these analyses. In the figure, the symbols are experimental data points, the thin black line is the analysis of the data using Eq. 3 (Supp. Eq. 15), and the somewhat thicker cyan line represents the fit of the data using Eq. 4 (Supp. Eq. 16). As shown in the figure, the two fits are essentially superimposable, indicating that the values of $C_I(r_F)$, $C_Q(r_F)$, and $C_{IQ}(r_F)$, and hence, of K_d obtained from analytical ultracentrifugation are consistent with the values for K_d obtained from SPR.

Determination of $\bar{v}$ *for* $YAQ_{12}A$ *and* $5QMe_2$

For $YAQ_{12}A$, a value for $\bar{v}$ was calculated as 0.679 cm^3/g, using the public domain software program SEDNTERP (http://www.rasmb.bbri.org/) developed by Hayes, Laue, and Philo (see also reference *27*). Solvent density was measured by standard volumetric techniques. To obtain $\bar{v}$ for $5QMe_2$, we performed sedimentation equilibrium of this peptide alone at three concentrations (100, 500 and 1000 μM), and at three angular velocities (36000, 48000, and 60000 rpm). Size exclusion chromatography shows this peptide to be predominantly or entirely monomeric at these concentrations. In addition, if one made the temporary assumption of an approximate value of $\bar{v}$ for this peptide of 0.7 cm^3/g, the calculated molecular weight in preliminary experiments was also most consistent with the monomer. For these reasons, we can use the monomeric molecular weight of $5QMe_2$ to calculate a more accurate value of $\bar{v}$ for subsequent sedimentation equilibrium experiments. At each concentration of $5QMe_2$ and angular velocity listed above, a plot of r^2 versus ln(absorbance) gave parallel straight lines for all three concentrations (Supporting Figure 1). The slope of these lines yielded a narrow distribution of values for the buoyant molecular weight, $M_b = M(1- \bar{v}\rho)$, of 310.96 ± 13.21 (mean ± standard deviation). Using this procedure, the values obtained for $\bar{v}$ were a narrow distribution of values, 0.681 ± 0.0135 cm^3/g (mean ± standard deviation).

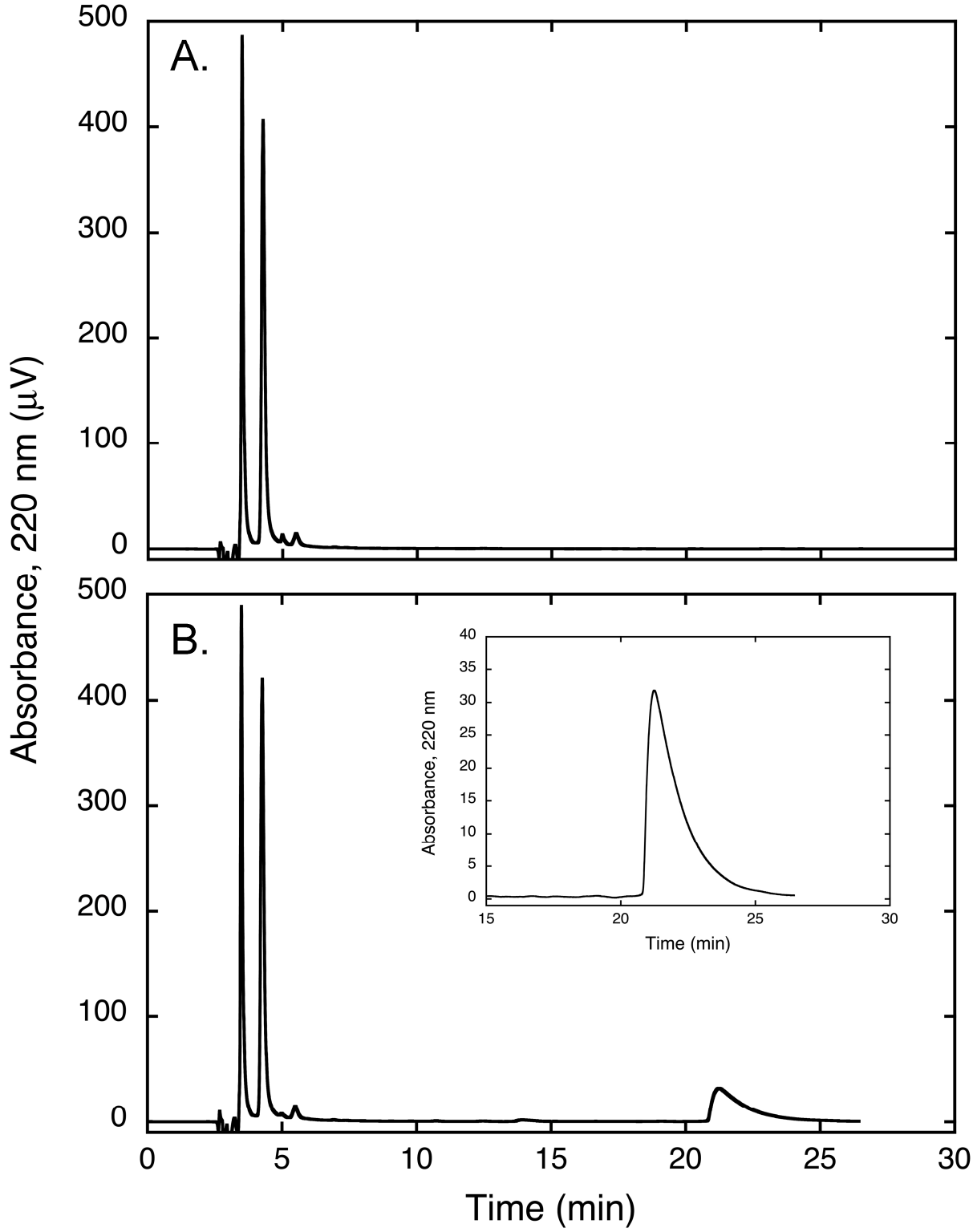

Supporting Figure 1. Isocratic analysis of $YAQ_{12}A$ remaining in solution, in the presence or absence of $5QMe_2$. Aliquots of soluble $YAQ_{12}A$ alone (A) or $YAQ_{12}A$ with $5QMe_2$ (B) were

injected onto a Zorbax C18 column. Column eluant was water:acetonitrile:TFA = 87.5:12.5:0.1 (v:v:v). Flow rate was 1.0 mL/min; column effluent was monitored at 220 nm. The inset in panel B shows the late eluting peak for $5QMe_2$.

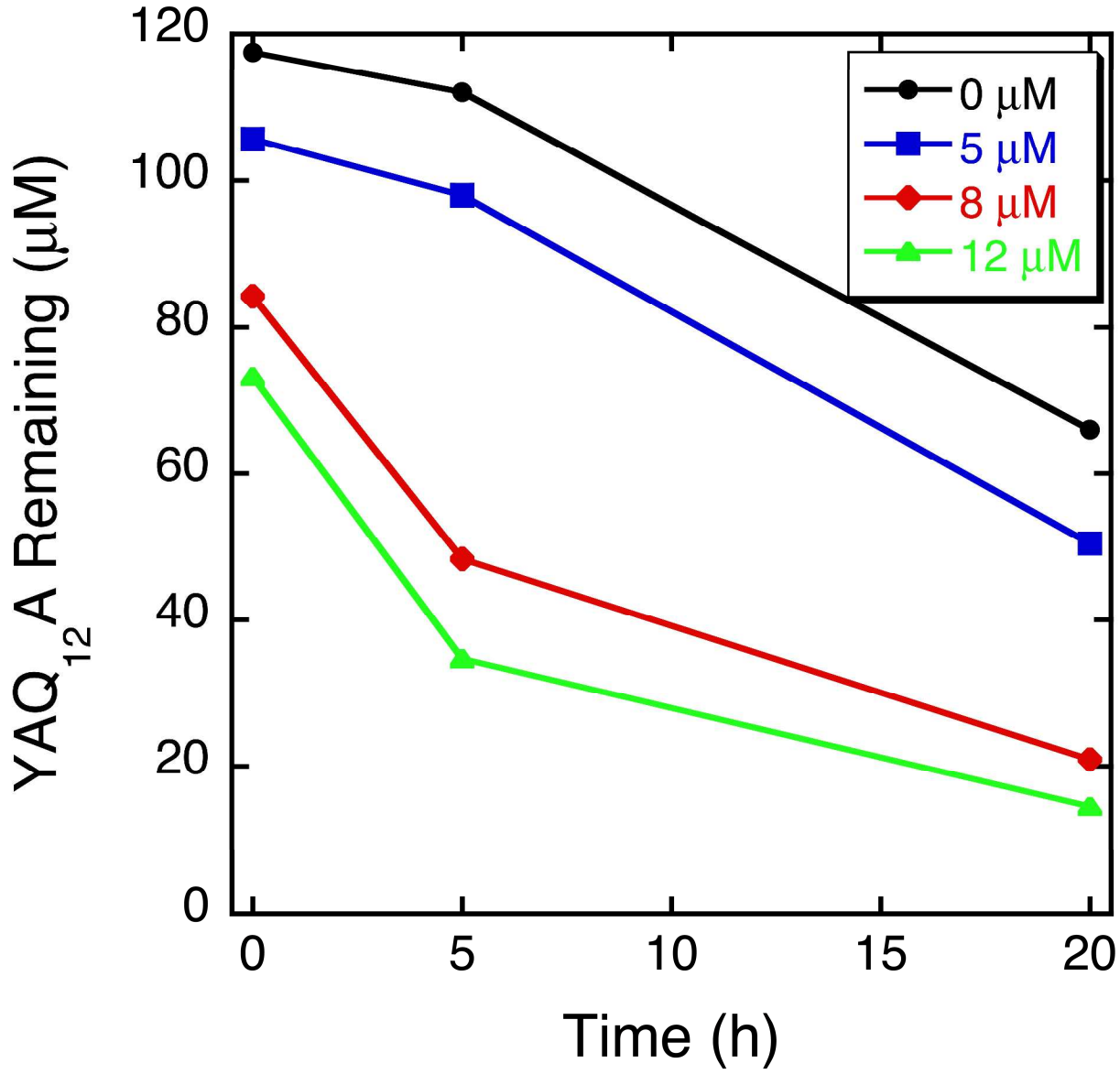

Supporting Figure 2A. Effect of added fibril seeds on fibrillation of $YAQ_{12}A$. $YAQ_{12}A$ at approximately 100 μM was incubated at 37 °C in 10 mM sodium phosphate (pH 7.40) either in the presence or absence of added $YAQ_{12}A$ fibril seeds. The amount of seed added is expressed as a nominal concentration of $YAQ_{12}A$ in the fibril seed slurry. At 0, 5, and 20 h, samples were analyzed for $YAQ_{12}A$ remaining in solution by the sedimentation assay described in Methods.

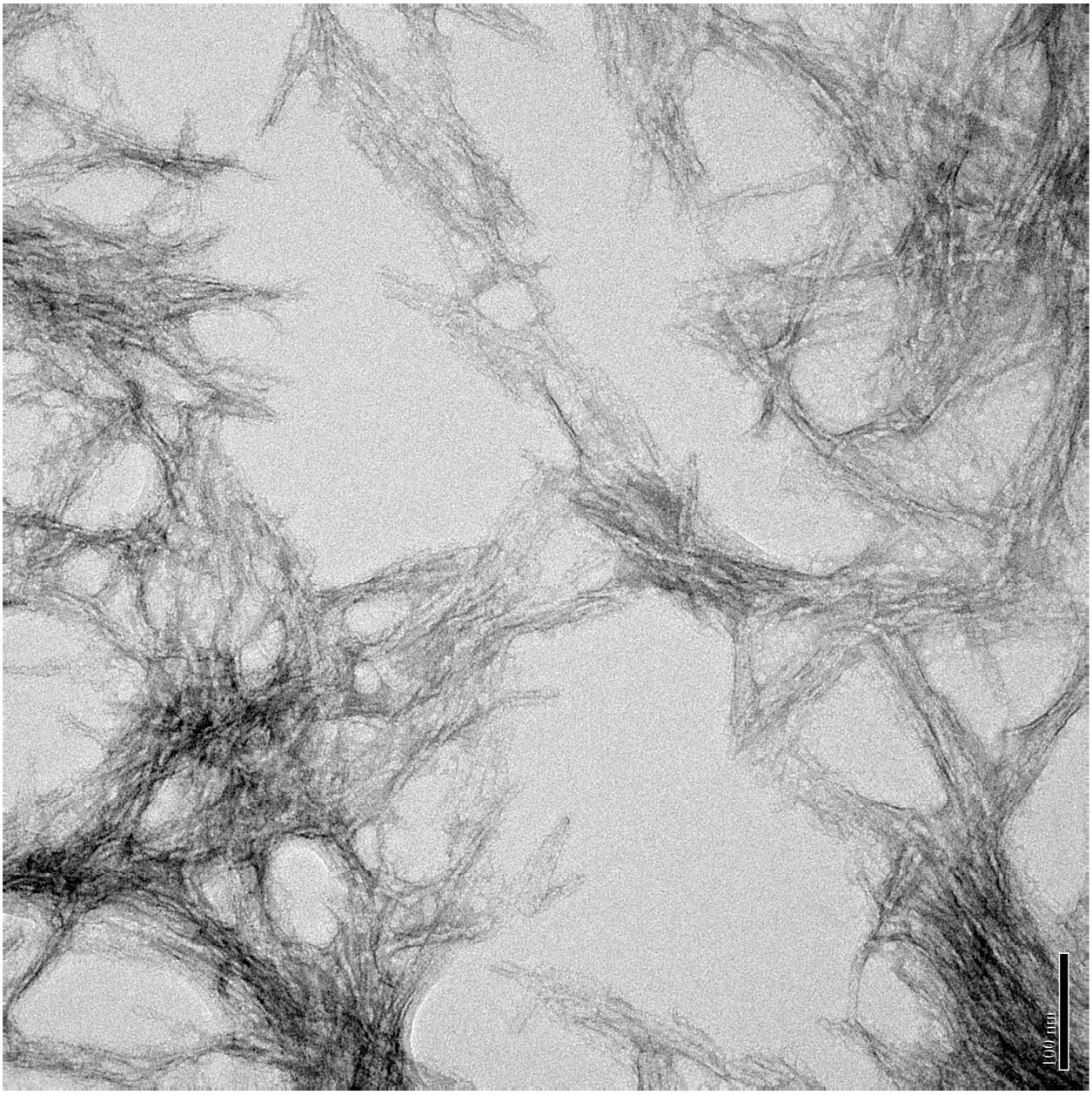

Supporting Figure 2B. Electron micrograph of fibril seed slurry, demonstrating that the peptide in this slurry was indeed fibrillar. Magnification is 49,000 ×, plus 1.4× magnification from the CCD camera.

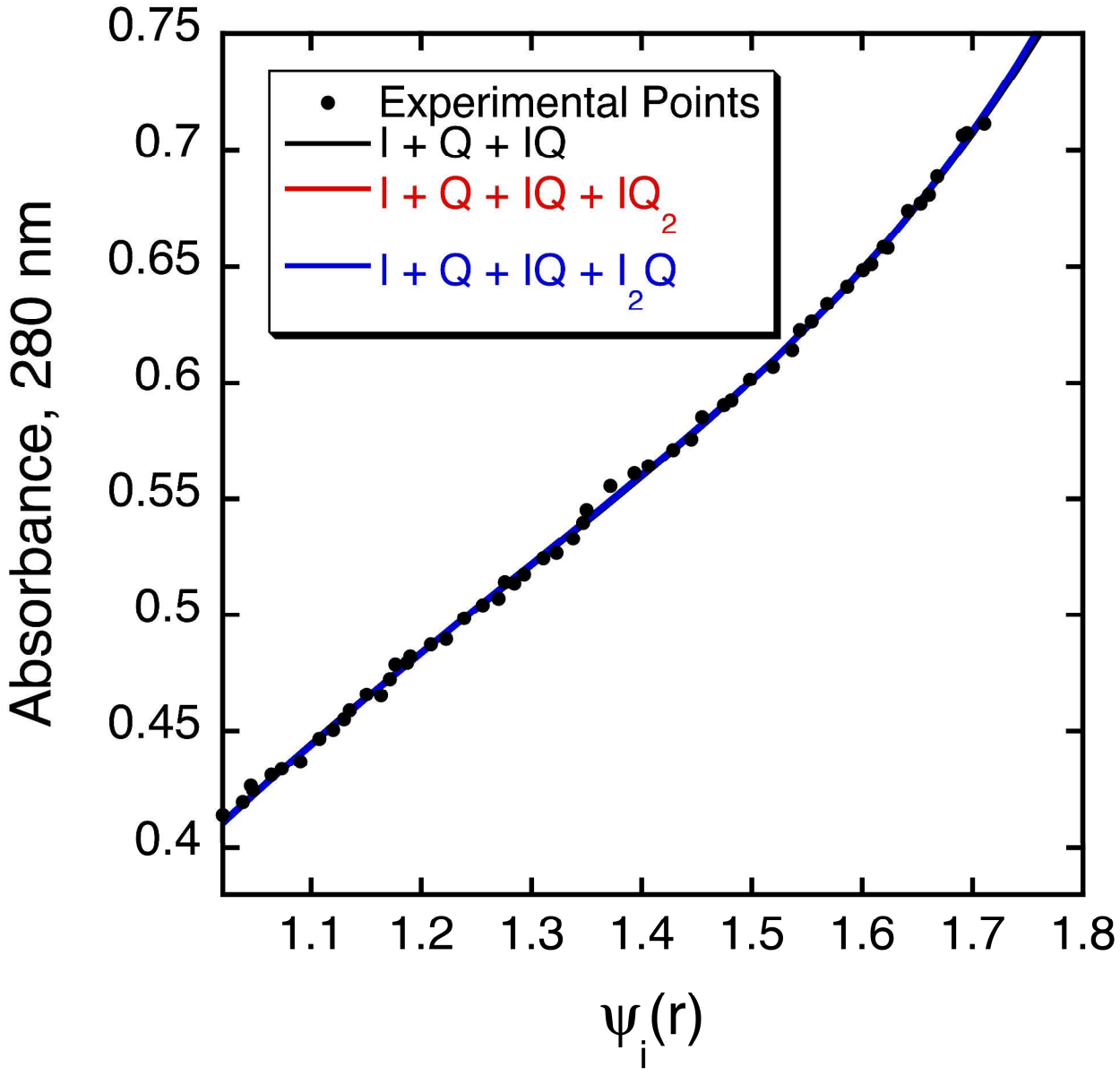

Supporting Figure 3. The example shown is for 100 µM $YAQ_{12}A$ and 1000 µM $5QMe_2$ centrifuged to equilibrium at 48,000 rpm, as described in Experimental Procedures. Figure 5 and Supporting Figure 3 shows a fit of the data to an equation containing terms for I, Q, and IQ; here, those data are reproduced (black line), and two additional fits are shown, one containing terms for I, Q, IQ, and IQ_2 (red line) and one containing terms for I, Q, IQ, I_2Q (blue line). The theoretical fits overlap completely (hence, not all colors are visible) and are indistinguishable from that obtained using the simpler equation.

Supporting Table 1: Comparison of Data Fits according to the Aikake Information Criterion

$5QMe_2$ (μM)	$YAQ_{12}A$ (μM)	ω (rpm)	AIC, No Complex	AIC, with Complex	Δ AIC
100	100	36,000	-412.86	-414.70	1.8433
100	100	48,000	-464.96	-466.22	1.2672
100	100	60,000	-438.05	-443.69	5.6486
500	100	36,000	-412.86	-414.70	1.8433
500	100	48,000	-467.37	-470.35	2.9761
500	100	60,000	-336.93	-443.69	106.77
1000	100	36,000	-414.86	-414.70	-0.16
1000	100	48,000	-464.96	-466.22	1.2672
1000	100	60000	-438.05	-443.69	5.6486

Sedimentation equilibrium analytical ultracentrifugation of mixtures of $5QMe_2$ and $YAQ_{12}A$ were performed and analyzed as described above, and in the main paper. The calculations in the table above are based on the data shown in Figure 5 of the main paper, in which the data were analyzed using Eq. 3; essentially identical results are obtained when the data are analyzed according to Eq. 4. The purpose of the calculations reported in the above table is to demonstrate that an equation containing a term for a complex is preferable to one in which there is no term for a complex between $5QMe_2$ and$YAQ_{12}A$. If $5QMe_2$ (I) and $YAQ_{12}A$ (Q) sediment independently of one another, without forming a complex, then the applicable form of Eq. 3 would be:

$$A_t(r) = C_I(r_F)\,\varepsilon_I\,\psi_I(r) + C_Q(r_F)\,\varepsilon_Q\,[\psi_I(r)]^p \qquad \text{Supp. Eq. 17}$$

If there is a 1:1 stoichiometric complex between $5QMe_2$ and $YAQ_{12}A$ (in addition to free $5QMe_2$ and $YAQ_{12}A$), then the applicable form of Eq. 3 would be:

$$A_t(r) = C_I(r_F)\,\varepsilon_I\,\psi_I(r) + C_Q(r_F)\,\varepsilon_Q\,[\psi_I(r)]^p + C_{IQ}(r_F)\,\varepsilon_{IQ}\,[\psi_I(r)]^{p+1} \qquad \text{Supp. Eq. 18}$$

The Aikake Information Criterion (AIC, see references *21* and *30*) was first proposed in 1974 as a measure of the goodness of fit of a statistical model. The most commonly used forms of the AIC are expressed either in terms of the residual sum of squares,

$$AIC_{SS} = n\left[\ln\left(\frac{SS}{n}\right)\right] + 2P$$

where n = number of data points, SS = residual sum of squares, and P = number of free parameters; or in terms of χ^2,

$$AIC_{\chi^2} = \chi^2 + 2P.$$

While it is generally to be expected that increasing the number of parameters will lower the sum of squares or χ^2, AIC not only "rewards" goodness of fit, but also "penalizes" the use of additional parameters to improve the goodness of fit, and this allows one to avoid overfitting data. Thus, AIC can be used to compared two or more models, with the best model being that with the lowest AIC value. As shown in the table above, in all cases but one, the AIC is lower for the form of the equation in which a term for a complex between $5QMe_2$ and $YAQ_{12}A$ is included. (In the case of the one exception, 1000 μM $5QMe_2$, 100 μM $YAQ_{12}A$, ω = 36,000 rpm, the two values for AIC are virtually identical.) These calculations suggest that the addition of a term for a complex (Supp. Eq. 18) does not go against the principle of parsimony and is the preferable model according to this criterion.

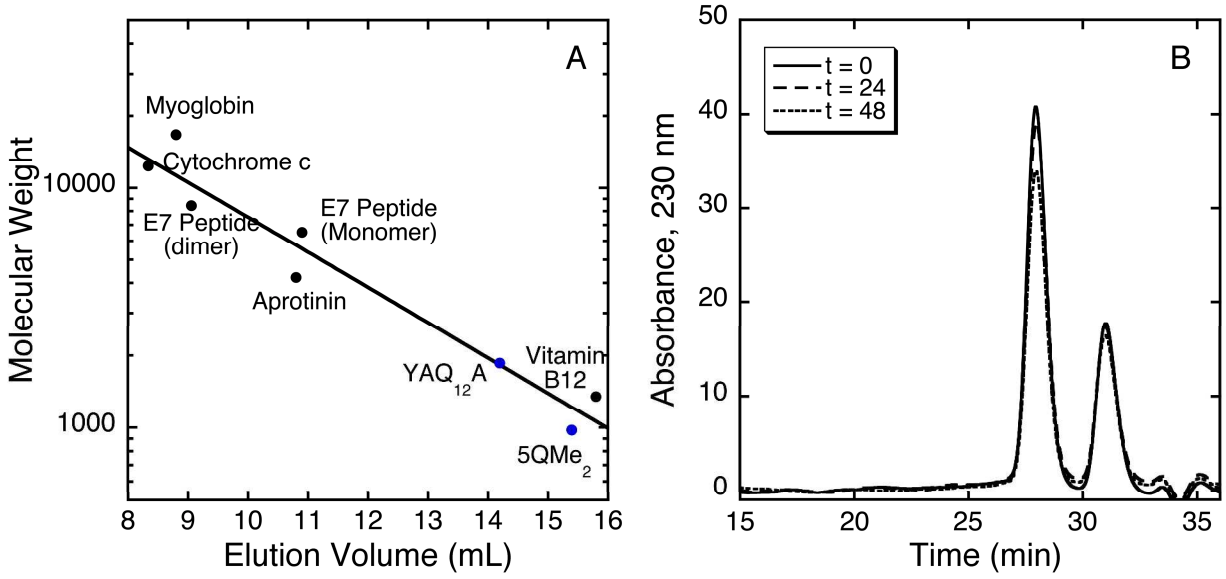

Supporting Figure 4. A. Calibration of Superdex Peptide 10/300 GL column. Mobile phase was the as used by the manufacturer, i.e., 0.02 mM sodium phosphate, 0.25 M NaCl, pH 7.20. Flow rate was 0.5 ml/min. The column effluent was monitored at 220 and 230 nm. Standards (molecular weights in parentheses) were horse myoglobin (16951.5), cytochrome c (12372), E7-peptide dimer (8431), aprotinin (6512), E7-peptide (4215.5), Vitamin B12 (1350), and Glycine (75). E7-peptide is from the E7 protein of human papillomavirus type 16. We synthesized it for other purposes using standard 9-fluorenylmethoxycarbonyl (FMOC) chemistry and Rink Amide resin, on an Applied Biosystems Model 431A peptide synthesizer, using essentially the same methods as described in the body of the paper. The amino acid sequence of the E7 peptide is:

NH_2-DSSEEEDEIDGPAGQAEPDRAHYNIVTFCCKCDSTLRL-COOH.

Mass of the monomer was verified by MALDI-TOF mass spectrometry (m/z=4216.85, expected = 4215.50). From these standards, we obtained a non-linear least squares fit to the equation log(MW) = -0.147*Ve + 5.344. From this equation, we obtained a MW^{app} = 1805.5 for $YAQ_{12}A$ (actual MW = 1860), and MW^{app} = 1176.0 for $5QMe_2$ (actual MW = 976). Although

the accuracy of determining molecular weight by size exclusion chromatography is limited, our data are most consistent with a monomeric state of both peptides.

B. Absence of a Small Zone Effect in SEC. As discussed in the body of the paper (see Figure 2F and G), when 100 μM $YAQ_{12}A$ and 170 μM $5QMe_2$ were loaded onto a Superdex Peptide 10/300 GL column, both peptides eluted in peaks of the same size and at the same elution time as when the peptides were loaded separately. No separate peak for the complex was present, apparently indicating complete dissociation of the complex during chromatography. If the complex between $YAQ_{12}A$ and $5QMe_2$ were long-lived, and $K_d \sim 1$ μM, one might expect to see a separate peak for the complex. As discussed in the paper and below, we attributed the lack of a peak of the complex to rapid dissociation of the complex. One additional possible explanation for not observing a complex peak, however, is a small zone chromatographic effect (Supporting References S1-S5). If such an effect had occurred, one would expect to observe a different chromatographic pattern upon changing the flow rate or the concentration of peptides, among other variables. This did not occur, however. We repeated this experiment but with a mixture containing 10 μM each of $YAQ_{12}A$ and $5QMe_2$. As shown in the figure (panel B), the two peaks eluted from the column at the same position observed for each of the peptides chromatographed alone.

The absence of a complex peak that persisted through chromatography underscores the transient nature of the complex between these two peptides, and the chaperone-like action of $5QMe_2$. Although the peptide mixture, when loaded onto the column, contains complex (as indicated by SPR and AUC data), as the peptides course through the column, the complex continually dissociates, and the zones of the two peptides are separated from each other chromatographically, i.e., due to their different molecular weights. Therefore, the concentration

of $5QMe_2$ *within the zone of* $YAQ_{12}A$ becomes very low – and similarly, for the concentration of $YAQ_{12}A$ within the zone of $5QMe_2$. In addition, both peptides get diluted as they pass through the column. For these reasons, we expected, and observed that at 0 and 24 h, both the size and elution position of the two peaks do not change compared with the peaks of each peptide chromatographed alone, and the two peptides elute from the column as completely separated peaks. At 50 h, there is a decrease in the size of the $YAQ_{12}A$ peak, consistent with our other observations that $YAQ_{12}A$ belatedly starts to form fibrils at this inhibitor concentration.

Supporting References

S1. Chun, P. W. and Yang, M. C. K. (1978) Scanning molecular sieve chromatography of interacting protein systems. Simulation of large zone behavior for self-associating solutes undergoing rapid chemical equilibration under kinetic control, *Biophys. Chem. 7*, 347-365.

S2. Chun, P. W. and Yang, M. C. (1978) Scanning molecular sieve chromatography of interacting protein systems. Effect of kinetic parameters on the large zone boundary profiles for local equilibration between mobile and stationary phases, *Biophys J. 24*, 56-57.

S3. Stevens, F. J. (1986) Analysis of Protein-Protein Interaction by Simulation of Small-Zone Size-Exclusion Chromatography: Application to an Antibody-Antigen Association, *Biochem. 25*, 981-993.

S4. Stevens, F. J. (1989) Analysis of protein-protein interaction by simulation of small-zone size exclusion chromatography. Stochastic formulation of kinetic rate contributions to observed high-performance liquid chromatography elution characteristics. *Biophys. J. 55*, 1155-1167.

S5. Wilton, W., Myatt, E. A., and Stevens, F. J. (2005) Analysis of Protein–Protein Interactions by Simulation of Small-Zone Gel Filtration Chromatography, *Methods Molec Biol*, *261*, 137-154.